Improved Speed Control of Permanent Magnet Synchronous Machine at Overmodulation Region

Yong-Cheol Kwon*, Sungmin Kim*, *Student Member, IEEE*, Tae-Suk Kwon**, *Member, IEEE* and Seung-Ki Sul*, *Fellow, IEEE*
*School of Electric Engineering & Computer Sciences, Seoul National University,
Seoul, Korea
**R&D Institute, Hyundai Mobis,
Yongin, Korea

***Abstract*—In Permanent Magnet Synchronous Machine (PMSM) drives, linear region, which is inside the inscribed circle of the voltage hexagon in the voltage plane, is mainly used for the stable operation. To enhance torque capability under the limited input DC link voltage, the region outside the inscribed circle of the voltage hexagon, known as overmodulation region, can be exploited in the flux-weakening operation. However, the operation of drive system in the overmodulation region cannot be free from the degradation of speed control performance. This paper presents investigations on control issues in the overmodulation region and proposes an algorithm for improving the speed control performance in the overmodulation region. The effectiveness of the proposed method is verified by computer simulations and experiments.**

I. INTRODUCTION

Recently, Permanent Magnet Synchronous Machines (PMSM) are adopted in many applications including traction and spindle drives. Because the main flux is supplied by the permanent magnet without additional coils, PMSM shows superior torque density and efficiency compared with other AC machines. And thanks to many efforts to expand operating speed, constant power operation above the base speed is realized in PMSM drive system. For the constant power operation, flux-weakening control for reducing stator flux linkage is generally used. Because the d-axis flux linkage is the sum of the flux linkage coming from the permanent magnet and that from Direct (d-) axis stator current, it can be weakened by applying negative d-axis current.

There have been many researches on the flux-weakening control [1]-[6] regarding PMSM drives. The main role of the flux-weakening controller is the determination of the current reference in the flux-weakening region. In accordance with operating conditions including operating speed, DC link voltage, and torque reference, the flux-weakening controller outputs a proper current reference. In most flux weakening algorithms [1]-[4], the voltage constraint is set- as the inscribed circle of the voltage hexagon. Although this up guarantees stable operation with low current harmonics, inverter capacity is not fully utilized by the flux-weakening method. In [5]-[6], an algorithm based on low pass filtered voltage difference signal is proposed. Using this method, overmodulation region is effectively utilized and torque capability of PMSM and inverter is resultantly increased by a few percents in the flux-weakening region. Though this method revealed satisfactory performance in torque control mode without an outer speed loop, it caused unexpected oscillations in the current with the outer speed control loop.

In this paper, speed control performance degradation of PMSM drive system in overmodulation region is investigated. Based on the analysis of control problems with the speed loop, a novel control scheme based on the voltage feedback is proposed. Applying the proposed method, speed control performance in overmodulation region is improved conspicuously in overall operating conditions. The effectiveness of the proposed scheme is tested with computer simulation and verified experimentally by an appropriate performance index defined for speed regulation performance evaluation.

II. CONVENTIONAL CONTROL SCHEMES IN PMSM DRIVES

A. Cascade Connected Speed Control System

Fig. 1 describes a general speed control system where the current regulator and speed regulator are connected in cascaded form. The current regulation loop is designed with the electric machine model and the speed regulation loop is designed with the system mechanical model under the assumption of ideal current regulation loop. Speed regulator produces the torque reference, T_e^*, from the given speed reference, ω_{rm}^*, and the actual speed, ω_{rm}. The rotor reference frame d-q current commands, i_{ds}^{r*} and i_{qs}^{r*}, are directly extracted from Maximum Torque Per Ampere (MTPA) pre-made look-up table and provided to the current regulator. Proportional-Integral (PI) controller in the rotor reference d-q frame [7] is employed as the current regulator, and an Integral-Proportional (IP) controller is used as the speed regulator. In this structure, the bandwidth of the current regulator, ω_{cc}, is designed higher enough than that of speed regulator, ω_{sc}, to prevent interference between the current regulator and the speed regulator. According to the general design rule, the bandwidth of inner control loop is set to be at least 5 times of that of the outer control loop. Applying the gains of the speed and the current regulators as explained in [7], the transfer

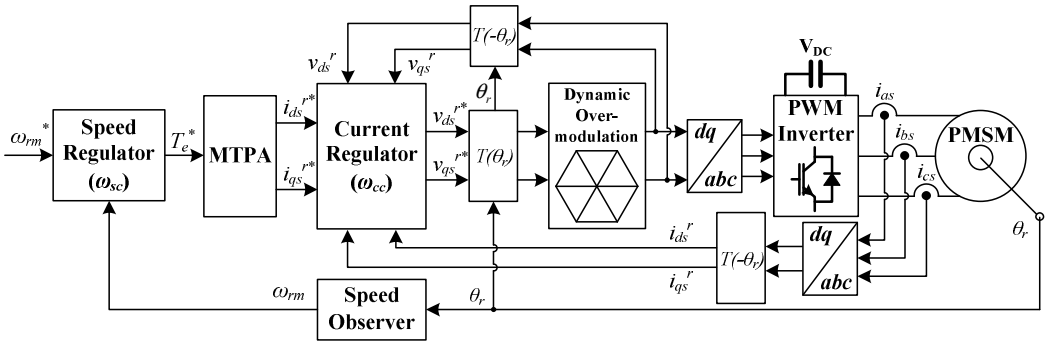

Figure 1. Cascade connected speed control system.

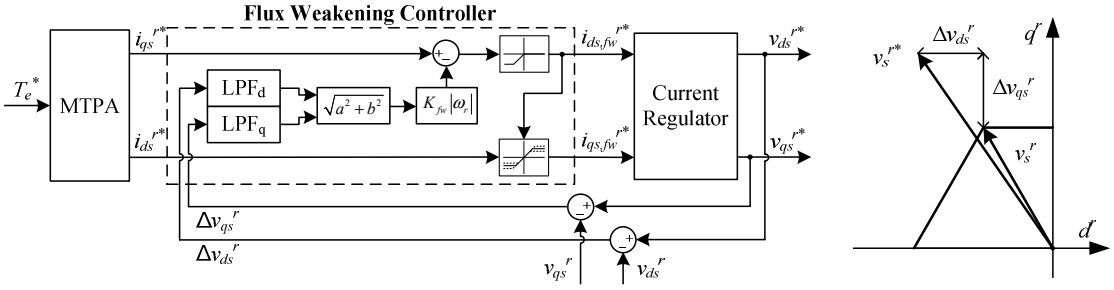

(a) Block diagram.

(b) Description of voltage difference terms.

Figure 2. Conventional flux-weakening controller for enhanced torque capability.

functions of the current regulation loop and the speed one can be derived as (1)-(2), respectively. The transfer functions in the current regulation loop can be assumed as a first order low pass filter like (1) and that of the speed regulation loop can be designed as a second order low pass filter where ζ is damping factor and ω_n is natural frequency as presented in (3).

$$i_{ds}^{r} = \frac{\omega_{cc}}{s+\omega_{cc}} i_{ds}^{r*}$$
$$i_{qs}^{r} = \frac{\omega_{cc}}{s+\omega_{cc}} i_{qs}^{r*} \quad (1)$$

$$\omega_{rm} = \frac{\omega_n^{\,2}}{s^2 + 2\zeta\omega_n + \omega_n^{\,2}} \omega_{rm}^{*} \quad (2)$$

$$\omega_n = \frac{\omega_{sc}}{\sqrt{\left(1-2\zeta^2\right) + \sqrt{4\zeta^4 - 4\zeta^2 + 2}}} . \quad (3)$$

B. Conventional Flux-weakening Method for Improved Torque Capability

In Fig. 2, a simplified block diagram is shown, which is the recently reported flux-weakening algorithm enhancing the torque capability of PMSM [5]-[6]. In Fig. 2, Δv_{ds}^{r} and Δv_{qs}^{r} indicate the voltage difference between the voltage reference from the current regulator and the assigned voltage to PMSM after dynamic overmodulation. LPF$_d$ and LPF$_q$ in Fig. 2 are Low-Pass-Filters which extract DC components of Δv_{ds}^{r} and Δv_{qs}^{r}. The key idea of this algorithm is increasing Modulation Index (MI) [8] for full utilization of the DC-link voltage of the drive system. For the flux-weakening executed by the voltage difference, the voltage reference vector from the current regulator should rotate outside the inscribed circle of voltage hexagon in the flux-weakening operation. So the overmodulation region in the voltage plane can be utilized and in turn, more torque can be produced within the rated current.

The flux-weakening gain, denoted as K_{fw}, is an important factor which enforces a trade-off between the transient current control performance and the torque capacity. As K_{fw} is decreased, the steady state voltage reference rotates through larger circle in the voltage plane, producing more torque. However, the transient performance of the current regulation is degraded because the voltage margin for the current regulation is deficient. Moreover, when the speed regulator is connected in series of the current regulator, more time is required to determine the torque reference to regulate the speed. So, for higher torque capability, which is realized by setting a low value for K_{fw}, the degradation of the transient control performance is unavoidable in the speed control system.

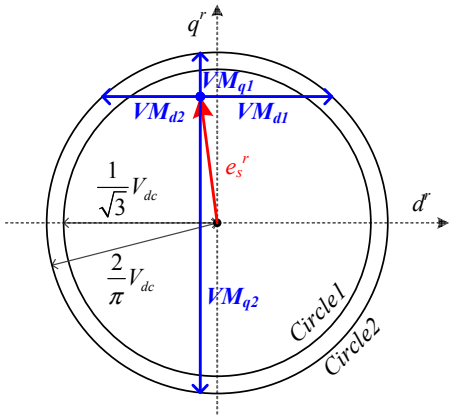

VM_{d1}: Voltage margin for increasing i_{ds}^r.
VM_{d2}: Voltage margin for decreasing i_{ds}^r.
VM_{q1}: Voltage margin for increasing i_{qs}^r.
VM_{q2}: Voltage margin for decreasing i_{qs}^r.

Figure 3. Definition of voltage margin.

III. Control Problems in Overmodulation Region

A. Voltage Margin Deficiency

If the rotating speed of PMSM is under the base speed, the transfer functions of current regulation can be expressed as in (1). However, with the flux weakening control in Fig.2, the transfer functions of the current regulation loop cannot be described as (1) because the steady state voltage reference is pushed to the overmodulation region as explained before. In the overmodulation region, the voltage reference from the current regulator cannot be generated due to the limited DC-link voltage. In this condition, the transient response of the current regulation is quite exacerbated. For intuitive understanding of this phenomenon, a concept of voltage margin introduced in [9] can be employed. The voltage equations of salient PMSM in synchronous reference frame are expressed as (4).

$$\begin{aligned} v_{ds}^{\ r} &= R_s i_{ds}^{\ r} + L_{ds}\frac{di_{ds}^{\ r}}{dt} + e_{ds}^{\ r} \\ v_{qs}^{\ r} &= R_s i_{qs}^{\ r} + L_{qs}\frac{di_{qs}^{\ r}}{dt} + e_{qs}^{\ r}, \end{aligned} \tag{4}$$

where $v_{ds}^{\ r}$ and $v_{qs}^{\ r}$ are the synthesized voltages by PWM inverter and $e_{ds}^{\ r}$ and $e_{qs}^{\ r}$ in (5), the effective back-EMFs induced by the rotation of the rotor.

$$\begin{aligned} e_{ds}^{\ r} &= -\omega_r L_{qs} i_{qs}^{\ r} \\ e_{qs}^{\ r} &= \omega_r (L_{ds} i_{ds}^{\ r} + \lambda_f) \end{aligned}. \tag{5}$$

At medium to high speed, the voltage drop across the resistance can be ignored. Then dynamic voltage is defined as the difference between the synthesized voltage and the effective back-EMF.

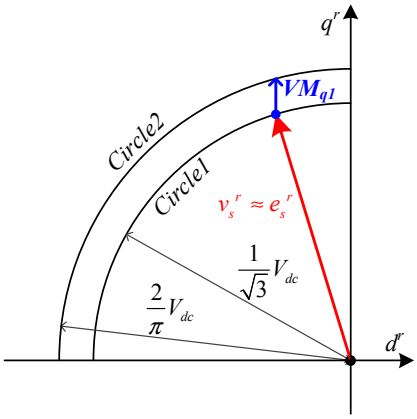

(a) Voltage constraint with only linear region [1]-[4].

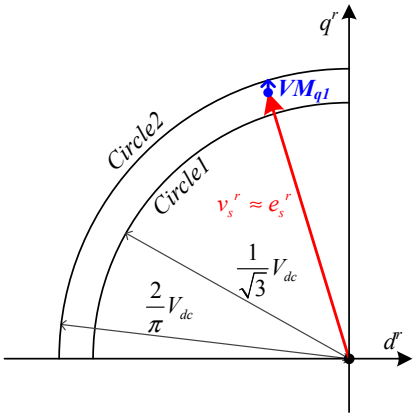

(b) Voltage constraint with overmodulation region [5]-[6].

Figure 4. Voltage constraints in different flux-weakenig methods.

$$\begin{aligned} v_{ds,dyn}^{\ r} &= v_{ds}^{\ r} - e_{ds}^{\ r} \approx L_{ds}\frac{di_{ds}^{\ r}}{dt} \\ v_{qs,dyn}^{\ r} &= v_{qs}^{\ r} - e_{qs}^{\ r} \approx L_{qs}\frac{di_{qs}^{\ r}}{dt}. \end{aligned} \tag{6}$$

The dynamic voltage is an important voltage which determines the actual variation of the current. For rapid variation of the current, the sufficient dynamic voltage is required to control the current. Using the minimum distance error overmodulation method, the output MI can be increased up to near $2/\pi \cdot V_{dc}$ which is accomplished by the six step operation [8]. And, the transient voltage constraint can be set as $2/\pi \cdot V_{dc}$. The magnitude of the dynamic voltage is dependent upon the gap between the voltage constraint and the effective back-EMF. This gap can be defined as a voltage margin for dynamic current regulation. In Fig. 3, four voltage margins are defined. Because the back-EMF coming from the permanent magnet, denoted as $\omega_r\lambda_f$, is located at the q-axis, the q-axis voltage is generally more deficient than the d-axis voltage.

Fig. 4 shows voltage constraints and voltage vector diagrams according to different flux-weakening methods

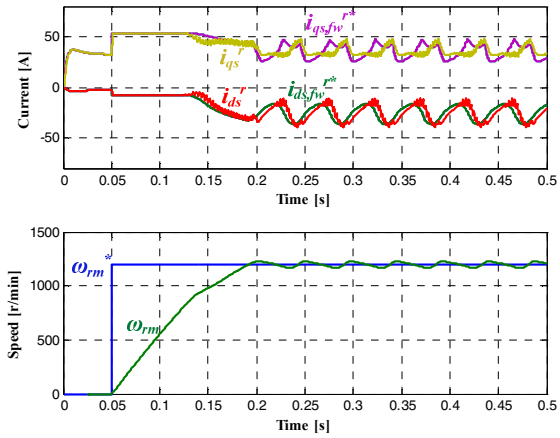

(a) Load torque: 0.6·T_{rated}, speed control bandwidth: 15Hz.

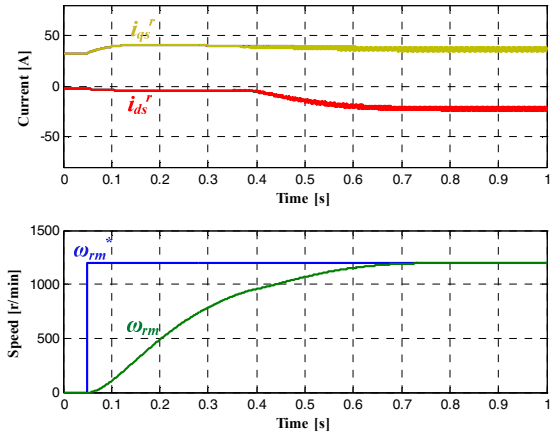

(b) Load torque: 0.6·T_{rated}, speed control bandwidth: 1Hz.

Figure 5. Simulation results: Speed regulation in different conditions.

when the motor is rotating in the positive direction. In Fig. 4, v_s^r and e_s^r are vector notations of the synthesized voltage and the effective back-EMF. Circle1 and Circle2 indicate linear region and the maximum voltage constraints accomplished by six step operation, respectively. Assuming that the motor is in the steady state and the voltage drop by the stator resistance is negligible, v_s^r can be approximated as e_s^r. When using only linear region, e_s^r is perched on circle 1. In this case, the overmodulation region is utilized only in the transient state and the voltage margin for increasing q-axis current, denoted as VM_{q1}, is relatively sufficient. Utilizing the overmodulation region, however, the steady state effective back-EMF is located between the circle1 and the circle2. In this case, because much portion of the overmodulation region is already exploited for maintaining the steady state current, VM_{q1} is very low. This is why the dynamic performance of the current regulation is deteriorated when the algorithm in Fig. 2 is used.

B. Speed Control Problem

Generally, due to the time delay in the current regulation, the bandwidth of the speed regulator is restricted. As described before, the bandwidth of speed regulator should be smaller enough than that of inner loop, the current regulation loop. In the overmodulation region, the current cannot be

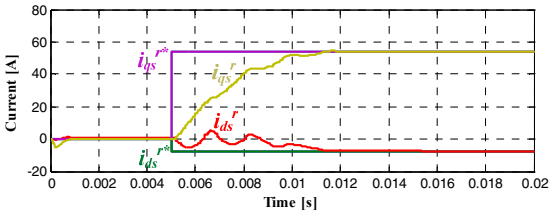

(a) Synchronous PI current regulator.

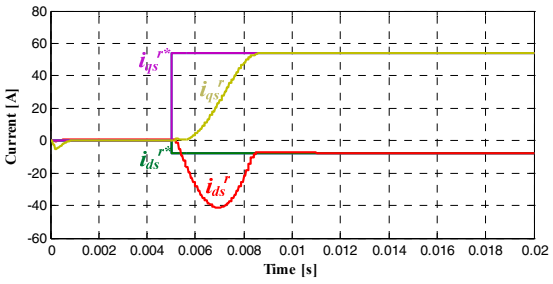

(b) Time optimal control.

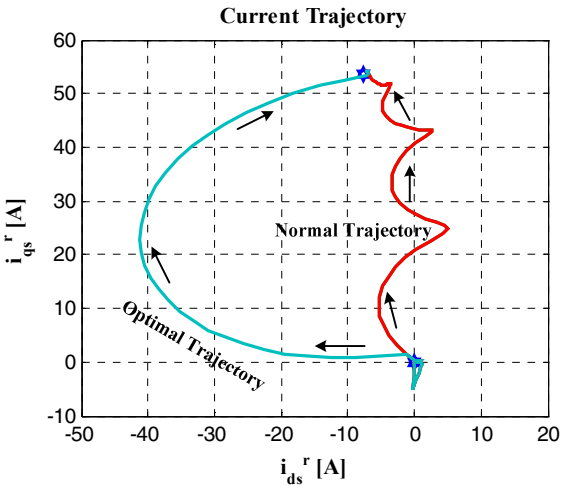

(c) Comparison of current trajectories.

Figure 6. Step responses of the current from differernt control methods.

regulated according to (1), but the regulation is far deteriorated. In the flux weakening region where the overmodulation is usually occurs, the bandwidth of the speed regulator cannot be set as that in the normal operation region under the base speed.

In Fig. 5, the simulation results of speed regulation in the overmodulation region with the control method in Fig.2 are shown. From standstill, the speed reference is set to 1200r/min with the constant load torque. System settings and motor parameters used for this simulation are shown in Table I. As shown in Fig. 5(a), the rotating speed is not well regulated, and continuously oscillates. This oscillation owes

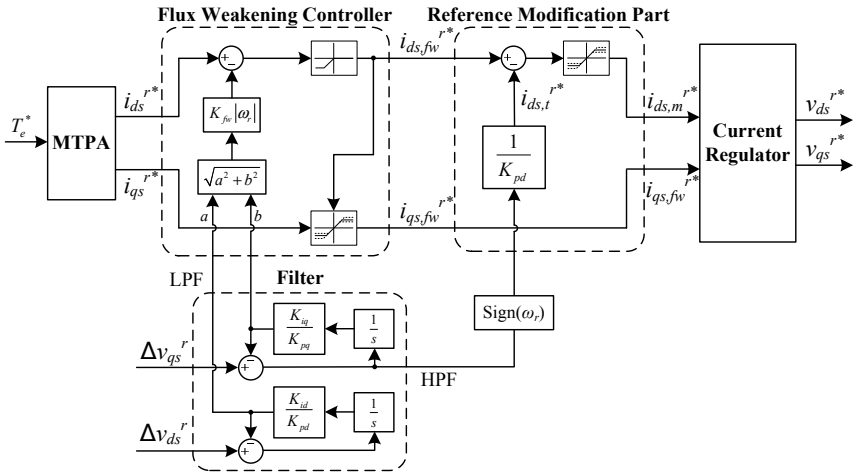

Figure 7. Proposed flux-weakening method.

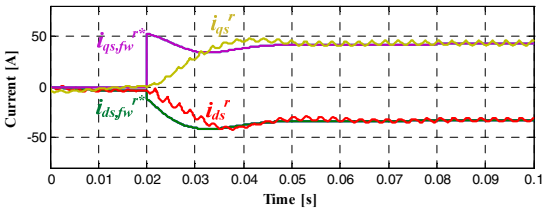

(a) Conventional method.

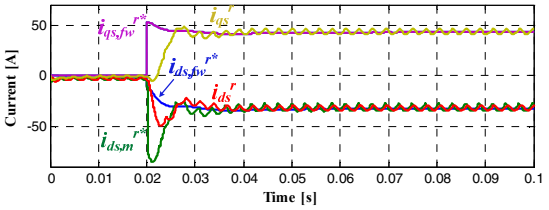

(b) Proposed method.

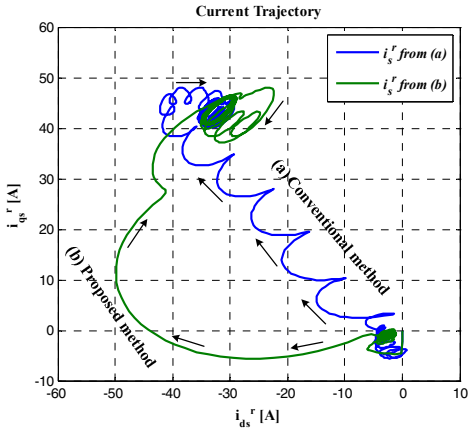

(c) Current trajectory of (a) and (b).

Figure 8. Simulation results: Current regulation.

to degraded current control dynamics. Because the transient current regulation performance is severely deteriorated, actual bandwidth of the speed regulation loop would be much lower than 15Hz, which is the set value in normal operating region. This causes the interference between the current regulator and the speed regulator and results in the oscillation. In Fig. 5(b), the results with 1Hz of speed control bandwidth is shown. In the steady state, the speed is well regulated according to the reference without any oscillation. However, 1Hz for the speed control bandwidth is not acceptable for the most of the drive applications because the speed regulation is too sluggish.

IV. Voltage Feedback Method for Improving Dynamics

To alleviate the steady state speed and current oscillation during the speed control, a novel control method, named voltage feedback method, is proposed [9]. Because the speed oscillation which is analyzed in the previous section comes mainly from the interference between the speed regulation loop and the current regulation loop, the oscillation can be reduced by enhancing the dynamics of the current regulation loop. Previous researches based on time optimal control theory [10]-[11] revealed that temporarily reducing d-axis current enhanced q-axis current regulation in the overmodulation region. Fig. 6 shows current trajectories from the optimal control and the PI control which are attained from simulations. In the simulations, the torque command is changed from zero to T_{rated} in the step manner. The optimal control reveals 43% reduction of settling time compared to the case of PI regulator in the overmodulation region.

But the implementation of the idea of time optimal control is too complicated to apply to PMSM drives in the industrial field. From the observation of the trajectories of the current on d-/q-axis current plane, a simple controller shown in Fig. 7 is proposed to mimic the optimal trajectory. The flux weakening method in Fig. 2 is incorporated in the proposed controller and the reference modification part is added to enhance the dynamics of the current regulation loop in the overmodulation region. When i_{qs}^{r*} is increased in step manner for the rapid acceleration at near or in flux weakening region, the voltage reference from the current regulator becomes larger than the voltage limit, defined as a hexagon in the

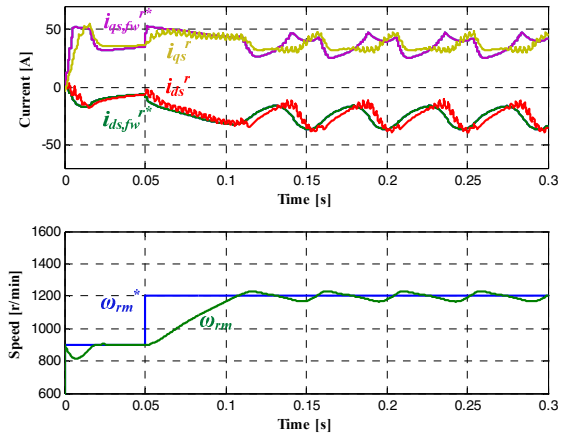

(a) Conventional method. Speed: 1200r/min, load torque: 0.6·T_{rated}, speed control bandwidth: 15Hz.

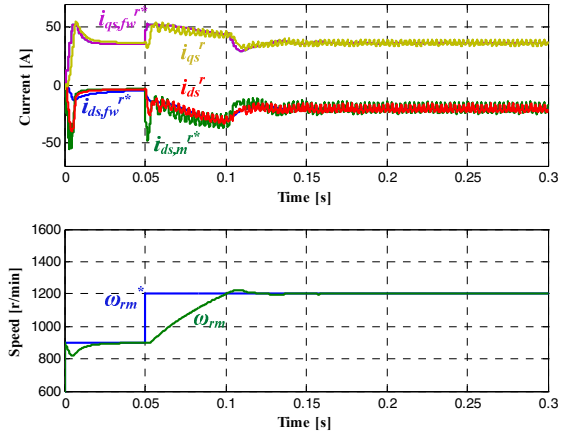

(a) Proposed method. Speed: 1200r/min, load torque: 0.6·T_{rated}, speed control bandwidth: 15Hz.

Figure 9. Simulation results: Speed regulation.

voltage plane. In this operating condition, the reference modification part modifies $i_{ds,fw}^{r*}$ from the high frequency component of Δv_{qs}^{r}, which is the voltage difference between the q-axis voltage reference and assigned q-axis voltage. In every operating condition, the reference modification part acts as securing more voltage margin in the transient state, which leads to improved current regulation performance. For the high pass filtered signal has no DC component in steady state, the transient reference modifier only works in transient state and the steady state operating current is only determined by the flux weakening controller.

The simulation results of current regulation in flux weakening region with and without the proposed controller are compared in Fig.8. The conditions and parameters of the simulation are shown in Table I. At 1200r/min, the maximum torque command is applied. Comparing Fig. 8(a) and Fig. 8 (b), it is evident that the proposed method shows conspicuously enhanced current regulation dynamics. In Fig. 8(b), the d-axis current reference is modified in the transient state so that the current moves through a short-cut. Physically, this d-axis current trajectory secures the additional q-axis

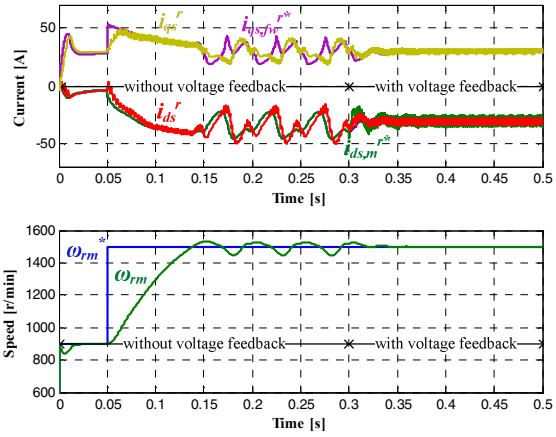

Speed: 1500r/min, load torque: 0.5·T_{rated}, speed control bandwidth: 15Hz.

Figure 10. Simulation results: Speed regulation.

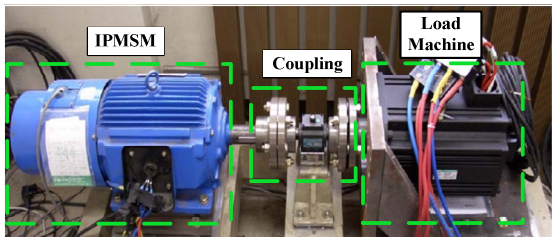

Figure 11. Experimental set-up.

voltage margin to control the q-axis current. The modification of the current trajectory is effectively visualized in Fig. 8(c).

Fig. 9 shows simulation results of speed regulation. The speed control bandwidth is set as 15Hz. With the conditions and parameters in Table I, speed reference is changed at t=0.05s. In Fig. 9(a), the speed reaches to the reference at t=0.11s but is not settled down, but continuously oscillates. In Fig. 9(b), using the proposed method, the speed increases even faster, crossing the reference value at t=0.1s. And, there is no oscillation in the speed but settled down to the reference value. This result proves that the proposed method improves the speed regulation performance.

In Fig. 10, another simulation of speed regulation is executed. The speed reference is changed at t=0.05s without the voltage feedback control. After t=0.3s, the proposed voltage feedback control is applied. As shown in Fig. 10, the current and speed oscillate when the voltage feedback is not applied. However, after 0.3s, the oscillation diminishes because the voltage feedback control improved the current control dynamics.

V. Experimental Verification

To prove the effectiveness of the proposed controller experimentally, a test set-up was prepared. Fig. 11 shows experimental set-up whose parameters and settings are the same as those in the cases of computer simulation given in Table I. Fig. 12 shows experimental results of speed

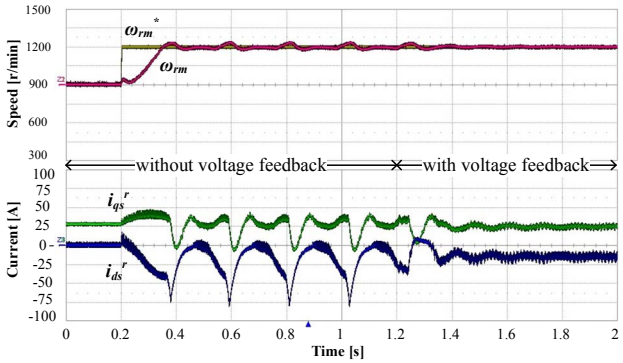

Figure 12. Experimental results: Speed regulation.

regulation with speed control bandwidth 15Hz. At the initial state, the speed command is set as 900r/min and the load torque is $0.5 \cdot T_{rated}$. At the first, without voltage feedback control, the speed reference is changed from 900r/min to 1200r/min in a step manner at t=0.2s. Even after the speed reaches 1200r/min, the responses of the speed and currents are oscillatory and not settled down even with some audible noises. At t=1.2s, the reference modification part proposed in this paper was engaged. Then the oscillations in speed and current response disappear. Because the d-axis current reference is properly corrected according to transient condition, the dynamics of the current regulation has been enhanced and the interference between the speed regulator and the current regulator is alleviated.

To evaluate the speed regulation performance, a performance index, denoted as PI_{sc}, defined as (7) is devised.

$$PI_{sc} = \frac{\omega_L}{s + \omega_L} |\Delta \omega_{rm}| \tag{7}$$

The performance index in (7) indicates DC component of the magnitude of steady state speed error, $\omega_{rm}^{*} - \omega_{rm}$. And, if the speed is regulated better, the performance index would be lower. Holding the speed reference at 1200r/min, PI_{sc} is calculated in various load conditions through the experiments. In these experiments, the maximum value of the speed control bandwidth ω_{sc} is set as 15 Hz. In Fig. 13(a) and (b), the experimentally obtained contours of the performance index according to the speed control bandwidth and the load torque are shown. And in Fig. 13(c) and (d), speed waveforms in specific operating condition A and B are drawn. Comparing Fig. 13(a) and Fig. 13(b), it is obvious that the speed control performance with the proposed controller has been conspicuously improved in overall operating conditions. The allowable design ranges where PI_{sc} is less than 1 r/min are compared in both cases with ω_{sc} and the load torque. For example, with the load torque under 30Nm, ω_{sc} is limited up to 3.6Hz with the conventional method. On the other hand, with the proposed control method, the bandwidth of the speed control loop can be set freely up to 15 Hz.

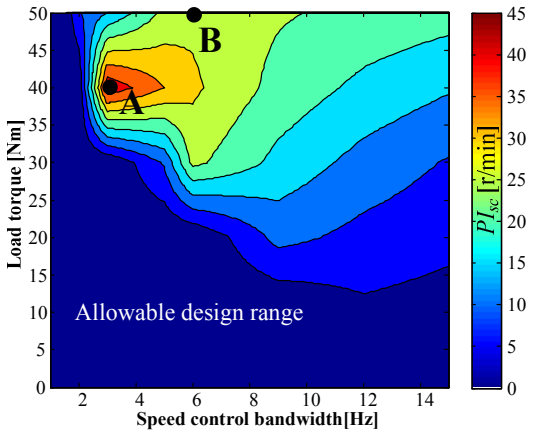

(a) Conventional method.

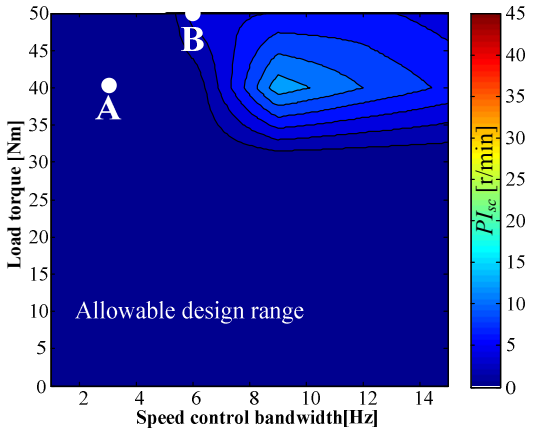

(b) Proposed method.

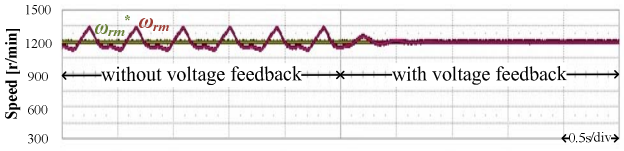

(c) Speed waveform in the condition A.

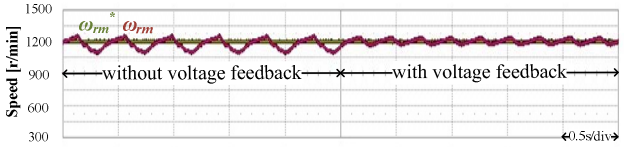

(d) Speed waveform in the condition B.

Figure 13. Performance index contours from experiments.

VI. Conclusion

In this paper, oscillatory speed responses in over-modulation region of PWM inverter are investigated. Because of the degraded current regulation dynamics in the region, interferences between the speed regulation loop and the current regulation loop occurs. As the result, the oscillations in speed and current responses occur. Because of these oscillations, the algorithm in Fig. 2 was not applicable in the applications where speed should be regulated by closed loop. To suppress the oscillation, voltage feedback method to enhance the dynamics of the current regulation loop has been

proposed. By applying the proposed method, the oscillation becomes smaller in overall operating condition, and the allowable speed control bandwidth has been increased conspicuously.

APPENDIX

TABLE I. SYSTEM SETTINGS AND MOTOR PARAMETERS.

Pre-designed current control bandwidth (ω_{cc})	500Hz
Current control period	100μs
Speed control period	1ms
DC-link voltage (V_{dc})	150V
Rated torque (T_{rated})	62N·m
Rated current (I_{rated})	39.5A_{rms}
Number of poles (P)	6 poles
Stator resistance (R_s)	0.15 Ω
Flux Linkage of permanent magnet (λ_f)	0.254V·s
D-axis inductance (L_{ds})	3.6mH
Q-axis inductance (L_{qs})	4.3mH

REFERENCES

[1] S. Morimoto, Y. Takeda, T. Hirasa, and K. Taniguchi, "Expansion of operating limits for permanent magnet motor by current vector control considering inverter capacity," *IEEE Trans. Ind. Appl.*, vol. 26, no. 5, pp.866 -871, Sept./Oct. 1990.

[2] S. Morimoto, M. Sanda, and Y. Y. Takeda, " Wide-speed operation of interior permanent magnet synchronous motors with high-performance current regulator," *IEEE Trans. Ind. Appl.*, vol. 30, no. 4, pp.920 -926, Jul./Aug. 1994.

[3] W. L. Soong and T. J. E. Miller, "Field-weakening performance of five classes of brushless synchronous AC motor drives," *Proc. Inst. Electr. Eng.*, vol. 141, no. 6, pt. B, pp. 331–340, Nov. 1994.

[4] J. M. Kim and S. K. Sul, "Speed control of interior permanent magnet Synchronous motor drive for the flux-weakening operation," *IEEE Trans. Ind. Appl.,* vol. 33, no. 1, pp. 43-48, Jan./Feb. 1997.

[5] T. S. Kwon and S. K. Sul, "Novel antiwindup of a current regulator of a surface-mounted permanent-magnet motor for flux-weakening control," *IEEE Trans. Ind. Appl.,* vol. 42, no. 5, pp. 1293-1300, Sept./Oct. 2006.

[6] T. S. Kwon, K. Y. Choi, M. S. Kwak, and S. K. Sul, "Novel flux-weakening control of an IPMSM for quasi-six-step operation," *IEEE Trans. Ind. Appl.,* vol. 44, no. 6, pp. 1722-1731, Nov./Dec. 2008.

[7] S. K. Sul, Control of Electric Machine Drive Systems, John Wiley & Sons, 2011.

[8] A. M. Hava, "Carrier-based PWM-VSI overmodulation strategies: analysis, comparison, and design," *IEEE Trans. Power Electron.*, vol. 13, no. 4, pp. 674-689, Jul. 1998.

[9] Y. C. Kwon, S. Kim, and S. K. Sul, "Voltage feedback current control scheme for improved transient performance of permanent magnet synchronous machine drives," *IEEE Tans. Ind. Electron*., in press.

[10] J. W. Choi and S. K. Sul, "Generalized solution of minimum time control in three-phase balanced systems," *IEEE Trans. Ind. Electron.,* vol. 45, no. 5, pp. 738-744, Oct. 1998.

[11] S. Bolognani, M. Tomasini, L. Tubiana, and M. Zigliotto, "DSP-based time optimal current control for high dynamic IPM motor drives," *Proc.IEEE 35th Annu. PESC*, Jun. 20–25, 2004, vol. 3, pp. 2197–2203.